

Effect of Ultrasound Immersion Freezing on the Quality Attributes and Water Distributions of Wrapped Red Radish

Bao-guo Xu · Min Zhang · Bhesh Bhandari ·
Xin-feng Cheng · Jincai Sun

Received: 17 November 2014 / Accepted: 23 February 2015 / Published online: 15 March 2015
© Springer Science+Business Media New York 2015

Abstract The microstructures, quality attributes (drip loss, firmness, sensory evaluation, and calcium content), and water distributions of ultrasound immersion frozen red radish (wrapped or unwrapped) were investigated. The results showed that ultrasonic treatment can significantly ($p < 0.05$) decrease the freezing time and better preserve the quality of frozen radish samples. In addition, ultrasound immersion frozen radish samples had smaller pore size and less destructive effect on microstructures from the scan electron microscopy (SEM) analysis. Wrapped radish had significantly ($p < 0.05$) lower calcium content, indicating that wrapped treatment was able to effectively prevent the solute uptake from the coolant to the radish samples. The water distributions of unwrapped samples were more uniform from the pseudocolor images of magnetic resonance imaging (MRI). Low-field nuclear magnetic resonance (LF-NMR) relaxation measurements showed that the vacuole water decreased, while the relative cytoplasm and intercellular space water increased under ultrasonic and unwrapped treatment.

Keywords Wrapped · Ultrasound · Immersion freezing · Quality · NMR · MRI · Red radish

B.-g. Xu · M. Zhang (✉) · X.-f. Cheng
State Key Laboratory of Food Science and Technology, Jiangnan
University, 214122 Wuxi, Jiangsu, China
e-mail: minlichunli@163.com

B. Bhandari
School of Agriculture and Food Sciences, The University of
Queensland, Brisbane, QLD 4072, Australia

J. Sun
Haitong Food Group Company, Zhejiang Cixi 315300, China

J. Sun
Zhejiang Pharmaceutical College, Ningbo 315100, China

Introduction

Red radish belonging to the Brassicaceae family is a cruciferous vegetable and has been cultivated in many countries, especially in China. Red radish is rich in anthocyanins, ascorbic acid, β -carotene, polyphenol, and flavonoid. These compounds are identified as highly nutritional and medicinal value and suggested as an alternative treatment for various ailments including hyperlipidemia, coronary heart diseases, cancer, and so on (Curtis 2003). However, fresh red radish has a limited shelf-life.

It is well known that freezing is one of the most effective preservation methods to maintain the original product properties such as nutrient contents, flavor, texture, and color. However, due to the high content of water in biological products, the water crystallization within the cells can cause serious expansion of the cellular volume, resulting in damages of the native cellular structure integrity (Cheng et al. 2014a). The extent of the damages mainly depends on the size and location of ice crystals which formed during freezing process. It is well known that the freezing rate largely affects the size and location of ice crystal in the tissue of frozen samples. Higher freezing rate is beneficial to the formation of smaller ice crystals, leading to slighter damages to the tissue and better preservation to the original quality (Ahmad et al. 2010; Ming et al. 2009; Streit et al. 2008). Thus, attempts have been made to improve the freezing rate and minimize the size of the ice crystals during the freezing process by ultrasonic treatment (Kiani et al. 2013b; Sun and Li 2003) and immersion freezing (Lucas et al. 1999; Lucas and Raoult-Wack 1998).

In recent years, power ultrasound has attracted considerable interest in food processing, such as extraction, emulsification, filtration, inactivation of microbial and enzyme, as well as thawing/freezing/crystallization (Bermúdez-Aguirre et al. 2011). As an assisted freezing technology, power ultrasound has been proved to be extremely useful in initiating

instantaneous nucleation process and also in the subsequent crystallization process (Chow et al. 2003, 2005; Kiani et al. 2011). The main effects, ultrasonic cavitation, and microstreaming of power ultrasound generate adequate mechanical, thermal, and chemical effects on food materials to enhance convective heat transfer during freezing process (Chandrapala et al. 2013; Kiani et al. 2013a; Sun and Li 2003; Zheng and Sun 2006). Therefore, ultrasonic treatment has been found to improve the freezing rate and decrease the size of the ice crystals during freezing process.

Immersion freezing (IF) in an aqueous refrigerating media consists of soaking foodstuffs in a cooled aqueous solution. IF is one of the fastest freezing techniques, as the heat transfer coefficient is up to 20 times higher in liquid media than that in air (Galletto et al. 2010; Lucas and Raoult-Wack 1998; Xin et al. 2014b). However, due to the problem of uncontrolled penetration of solutes into the food materials, IF has a limited application range (Lucas and Raoult-Wack 1998). In view of this disadvantage, special solution solutes for the coolant or treatments for the products need to be chosen to avoid solute uptake from the coolant into the products.

Many studies have been reported that ultrasound-assisted IF (UAIF) was applied to freeze many different kinds of food materials including potato (Comandini et al. 2013; Li and Sun 2002; Sun and Li 2003), sucrose solution (Chow et al. 2003, 2004, 2005; Hu et al. 2013a), apple (Delgado et al. 2009), agar gel (Kiani et al. 2011, 2012, 2013b), dough (Hu et al. 2013b), mushroom (Islam et al. 2014), broccoli (Xin et al. 2014a, b), red radish (Xu et al. 2014), and strawberry (Cheng et al. 2014b) and so on. These research works mainly focus on the freezing rate, nucleation temperature, and quality.

However, there is a lack of published information on the controlling of solute uptake and water distributions of red radish samples by UAIF in CaCl_2 solutions. Therefore, the main objectives of the current study are to evaluate the effect of wrapped and ultrasonic treatment on freezing time, drip loss, texture, and sensory evaluation of red radish cylinders frozen by IF. In addition, special attentions are also paid on the total and cell wall-bound calcium contents, the ratio of bound calcium/total calcium, microstructures, and water distributions of frozen red radish samples.

Materials and Methods

Raw Materials

Red radishes (Xin Ling Mei) harvested in May 2014 were provided by a farm (Weifang, Shandong province, China). Red radishes were selected according to internal color (uniform red) and washed in the tap water, drained, and dried with a fan. Then, they were cut into red radish cylinders with 2.5 cm in diameter and 3.0 cm in height using a regular steel

mold and stored in a refrigerator at 4 ± 1 °C for 6 h to achieve uniform initial temperature until used. The initial moisture content of these radish samples was $92.31 \% \pm 0.33 \%$ (w. b.).

Experimental Procedure and Design

A laboratory-scale ultrasound-assisted freezer (Ningbo Scientz Biotechnology Co., Ltd., Ningbo, China,) with 20-kHz frequencies and 0–300-W tunable electric power levels was used for red radish IF. The detailed parameters of the freezer were introduced in our previous research (Xu et al. 2014). The different freezing conditions included IF, UAIF, IF with wrapped treatment (IFW), and UAIF with wrapped treatment (UAIFW). The radish samples were tightly coated by polyethylene plastic wrap (0.5-mm thickness) to avoid contacting with coolant (namely, wrapped treatment). CaCl_2 solution (30 %, w/v) was used as freezing coolant.

During freezing process, the temperature of coolant for all the experimental runs was maintained at -20 ± 1 °C. The prepared radish cylinder samples (100 g for each batch) were removed from the refrigerator, and K-type thermocouple (1.0-mm diameter, accuracy ± 0.1 °C) with a digital thermometer (UT325 thermometer, Uni-Trend Technology Limited, Dongguan, China) was inserted into the geometric center of one of those radish samples. The gap between the thermocouple and radish was sealed by melted paraffin to prevent the solution penetrating into the radish samples. The inserted sample of each batch was specifically placed at the fixed chosen location for each experiment to avoid fluctuations of velocity at different position in the chamber. During the UAIF and UAIFW trials, the samples were irradiated by ultrasound waves with 20-kHz frequency, 30 s on/30 s off duty cycle, and 0.26-W/cm^2 intensity which was the optimal parameters in our previous studies. The calorimetric method was used to determine the actual dissipated acoustic power and acoustic intensity, as introduced in our previous research (Xu et al. 2014). The freezing process finished as soon as the temperature of the sample reached -18 °C.

After freezing, each frozen sample was immediately placed into a double high-density polyethylene bag and thawed in a constant temperature and humidity chamber (HWS-080, Shanghai Jinghong laboratory instrument Co., Ltd, Shanghai, China) maintained at 20 ± 0.5 °C and 70 ± 5 % RH. After thawing was completed (the temperature in the geometric center of the samples reached to 4 °C), the samples inside the polyethylene bag were kept in a 4 °C refrigerator for further measurements. Each freeze/thawing experiment was undertaken in triplicate.

Drip Loss Analysis

Drip loss was divided into freezing loss and thawing loss. The freezing loss was measured immediately by weighing each

sample before and after the freezing process and calculated as the percentage loss of initial weight using Eq. (1); the thawing loss was calculated using Eq. (2) provided by (Agnelli and Mascheroni 2002).

$$\text{Freezing loss} = (m_0 - m_1) / m_0 \quad (1)$$

$$\text{Thawing loss} = (m_3 - m_2) / m_1 \quad (2)$$

where m_0 and m_1 were the weight of the samples before and after freezing, m_2 (g) was the mass of dry blotting paper, m_3 (g) was the weight of wet blotting paper with exuded liquid.

Firmness Analysis

The firmness was measured by using a texture analyzer (TA-XT2 of Stable Micro Systems, Ltd., Surrey, UK) in compression mode with a 2-mm diameter cylindrical probe (SMS-P/2, Stable Micro Systems, Ltd., Surrey, UK). The operating parameters were pretest speed (2.00 mm/s), test speed (1.00 mm/s), posttest speed (5.00 mm/s), and trigger force (5.0 g). The samples were deformed 50 %. The force–deformation curves were recorded using a software provided by the manufacturer, and the maximum force (N) was calculated and used as firmness. Eight replicates were carried out.

Analysis of Total Calcium Content

The total calcium content of radish was analyzed by using atomic absorption spectrophotometry (AAS) method described by Kawashima and Valente Soares (2003) with slight modification. About 5 g of fresh or thawed radish samples was digested with 2 mL of 65 % HNO₃ solution and put into a muffle furnace at about 550 °C for 4 h. Residues were diluted to a proper concentration for measurement using AAS. Lanthanum solution and HNO₃ were added to reach a final concentration of 10 and 2 %, respectively. The solution obtained was used to determine calcium using a flame atomic absorption spectrometer (Spectr AA, Varian, Palo Alto, USA).

Analysis of Calcium Content of Alcohol-Insoluble Solids (AIS)

The calcium content of the alcohol-insoluble solids (AIS) was determined by the method of Galetto et al. (2010) with some modifications. Radish tissues (20 g) were cut, ground, and homogenized with 200 mL of 96 % (v/v) ethanol using a homogenizer at 16,000 rpm for 3 min. Then, the mixture was kept in a water bath at 80 °C for 30 min, and the ethanol was decanted by filtration. The residue was washed and

filtrated using 200 mL of 80 % (v/v) ethanol until total whitening, and then dried in oven at 40 °C. The obtained residue was the AIS, and the calcium content of AIS samples was determined by using the same procedure as was used for determining total calcium content.

Scanning Electron Microscopy Analysis

The frozen radish cylinders were freeze-dried in a freeze-dryer (Model 77530-30, Labconco Co., USA) to prepare sample for scanning electron microscopy (SEM) analysis. Dried samples were placed on one surface of a two-sided adhesive tape. Gold preprocessing was performed under vacuum conditions and then observed on a Quanta-200 scanning electron microscope (SEM, Quanta-200, FEI, Netherlands).

Nuclear Magnetic Resonance and Magnetic Resonance Imaging Analysis

A low-field pulsed PQ001 analyzer (Niumag Electric Corporation, Shanghai, China) with 18.2 MHz was used in these experiments to determine the distribution and status of water in freeze-thawed radish cylinders. Approximately 7 g of radish sample was placed in a 25-mm glass tube and inserted in the NMR probe. The height of measurements was controlled in 20 mm. Carr–Purcell–Meiboom–Gill (CPMG) sequences were employed to measure the transverse time (T_2). Typical pulse parameters were as follows: P90=5 us, P180=10 us, TD=505,528, SW=100 KHz, D3=80 us, DR=1, TR=16,000 ms, RG1=10, DRG1=3, NS=4, DL1=0.5 ms, NECH=5000. Each measurement was performed in triplicate.

The 2D proton density images from transverse section of samples by different freezing conditions were analyzed by the MRI. Typical pulse parameters were as follows: TE=18.2 ms, TR=2000 ms, matrix size=256×256, FOV=10 cm×10 cm, slice width=2.5 mm, and slices=4. In order to investigate the water distributions at different positions inside the radish, the images of each 6-mm layers of samples were taken.

Sensory Evaluation

Sensory analysis of fresh and thawed red radish samples was carried out according to the method described by Hajare et al. (2006) with some modifications. An expert panel of 12 (4 M, 8 F) nonsmoking, self-confessed healthy researchers/scientists were scientific staffs from School of Food Science and Technology, Jiangnan University. Panelists were trained to align their quality perception and scores in terms of appearance, aroma, flavor, and texture of fresh and thawed radish before actual testing. Sensory evaluation was conducted in individual booths of a sensory tasting laboratory under the controlled environment. The blind tasting and centesimal score system was applied to evaluate the radish's quality.

The score distributions were appearance (25 scores), aroma (25 scores), flavor (25 scores), and texture (25 scores). Samples with a total score of below 70 were considered as unacceptable, between 70 and 80 were common, over 80 were good and acceptable, and over 85 were excellent. The results obtained were analyzed using statistical tools like mean and standard deviation.

Statistical Analysis

Statistical analysis of variance (ANOVA) was performed using SPSS 20.0 software (IBM, Chicago, IL, USA). The significant difference between two means was determined by using Tukey's test procedure at 95 % confidence level ($p < 0.05$).

Results and Discussion

Freezing Curves and Freezing Time Distributions

The freezing time–temperature profiles of red radish cylinders under different freezing conditions are depicted in Fig. 1. It can be clearly seen from this figure that different freezing conditions resulted in different freezing times. UAIF had the shortest freezing time, followed by IF and UAIFW, while the freezing time of IFW was the longest. Compared to the UAIF and IF, the freezing times of UAIFW and IFW were longer. This was mainly because the wrapped treatment blocked the direct contact of coolant and samples, leading to the decrease of heat transfer. In addition, the freezing times of UAIF and UAIFW were still shorter than those of IF and IFW, respectively. This result distinctively showed that ultrasonic treatment can decrease the freezing time. This was attributed to

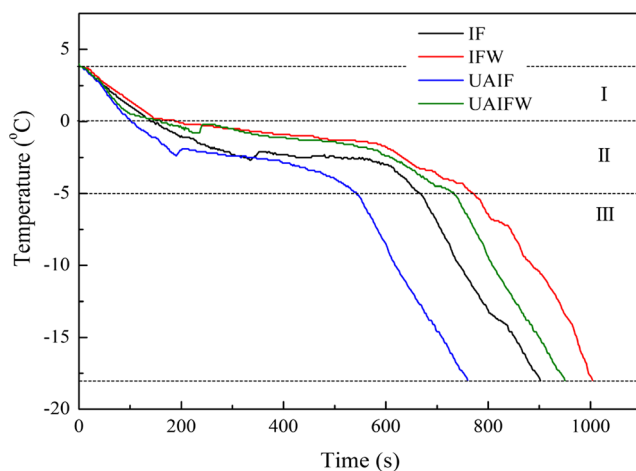


Fig. 1 The freezing curves of radish cylinders under different freezing conditions. IF (immersion freezing), IFW (immersion freezing with wrapped treatment), UAIF (ultrasound-assisted immersion freezing), UAIFW (ultrasound-assisted immersion freezing with wrapped treatment)

the fact that the power ultrasonic waves propagated into the coolant and samples' surface through plastic wrap and cavitation phenomenon took place. During this process, a large number of cavitation bubbles were generated, and these tiny bubbles sometimes can act as crystal nucleus which induced primary ice nucleation (Kiani et al. 2011; Saclier et al. 2010). Also, the collapse of some bubbles could produce a cataclysmic event-local zones of extremely high pressures (70–100 MPa) resulting in supercooling of solution; supercooling effect could also play the role of an instantaneous nucleation driving force (Inada et al. 2001; Xu et al. 2014). Additionally, a large amount of stable ultrasonic cavitation bubbles could move, causing the formation of microstreaming. The microstreaming could also induce the ice nucleation (Hu et al. 2013b). Moreover, the propagation of ultrasonic waves into the fluid resulted in macroscopic turbulence flows causing an increase in high-speed collision frequency of microscopic particles. As a result, the solid–liquid boundaries became thinner, and the heat transfer resistance decreased (Hu et al. 2013b; Xin et al. 2014b). Consequently, the ultrasonic treatment in freezing can induce ice nucleation and improve heat transfer to shorten the freezing time.

As can be seen from the Fig. 1, all the freezing curves can be roughly divided into three different stages: precooling stage (4 to 0 °C, stage I), phase change stage (0 to -5 °C, stage II), and subcooling stage (-5 to -18 °C, stage III). The required times for each stage of freezing process are shown in Fig. 2. It shows that different freezing conditions had different freezing time distributions at each stage. Concerning the time required at the precooling stage, UAIF and IF were quite shorter than those of UAIFW and IFW. This was justified with the insulation effect of heat transfer by the wrapped treatment. In addition, the precooling stage of UAIF was shortest. It is well known that the phase change stage is the most important stage during freezing process, because the ice crystals of samples are mainly generated in this stage. Shorter freezing time in this

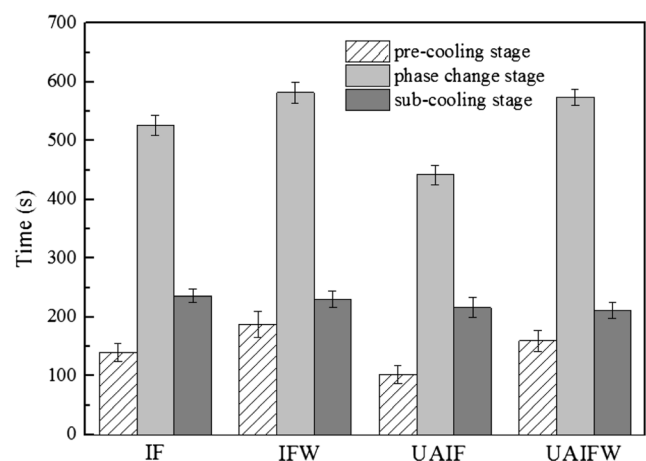


Fig. 2 The time spent on each freezing stage under different freezing conditions. Bars represent mean±standard deviation of triplicates

stage is crucial to obtain frozen food samples with higher quality (Delgado and Rubiolo 2005; Xin et al. 2014a). From the Fig. 2, it is shown that UAIF had a remarkable effect on shortening the phase change stage. This was due to the induction of ice nucleation and improvement of heat transfer during freezing process by the ultrasonic treatment. Additionally, no obvious difference of freezing time in this stage was observed between IFW and UAIFW. Regarding the time required at the subcooling stage, there were no distinct differences among those different freezing conditions.

Total Calcium Content and Calcium Content in the Alcohol-Insoluble Solids

The reason why the IF technology with extremely high freezing rate cannot be widely used was because of the uncontrolled solute uptake from the liquid coolant into the product during the freezing process (Lucas and Raoult-Wack 1998; Xin et al. 2014b). In food processing, calcium is always applied to harvested fruits and vegetables to retard the softening, reduce the decay rate, and prolong the shelf-life. This is because the calcium in cell wall is a key factor to maintain cell wall structure and integrity. However, too much calcium uptake from the liquid coolant into the product may affect the taste of the fruits and vegetables. Therefore, wrapped treatment was carried out in this study to avoid samples contacting to coolant.

As can be seen from Table 1, there were no significant differences ($p>0.05$) of total calcium content among fresh samples, IFW and UAIFW samples. The total calcium content of UAIF and IF samples in CaCl_2 solutions increased significantly ($p<0.05$), which were nearly 10 times higher than those of fresh samples, UAIF and IF samples. This result indicated that the wrapped treatment prevented the CaCl_2 coolant solutes from penetrating into the radish tissues effectively. Moreover, compared to IF, the total calcium

Table 1 Total calcium content, calcium content in the alcohol-insoluble solids (AIS), and the ratio of bound calcium/total calcium of fresh and thawed radish cylinders under different freezing conditions

Treatments	Total calcium content (mg/100 g)	Calcium content in the AIS (mg/100 g)	Ratio of bound calcium/total calcium
FR	57.20±2.61 ^c	40.07±2.33 ^c	0.70±0.04 ^a
IF	528.85±6.14 ^b	259.01±5.12 ^b	0.53±0.06 ^c
IFW	50.33±3.62 ^c	21.07±2.11 ^d	0.42±0.03 ^e
UAIF	566.09±7.55 ^a	322.90±3.78 ^a	0.57±0.07 ^b
UAIFW	52.41±3.89 ^c	25.07±2.93 ^d	0.48±0.05 ^d

Values with different lowercase letters in the same column are significantly different ($p<0.05$). Results are mean±standard deviation ($n=3$)

content of UAIF samples was higher. Similar result was also reported by Xin et al. (2014b) for broccoli samples.

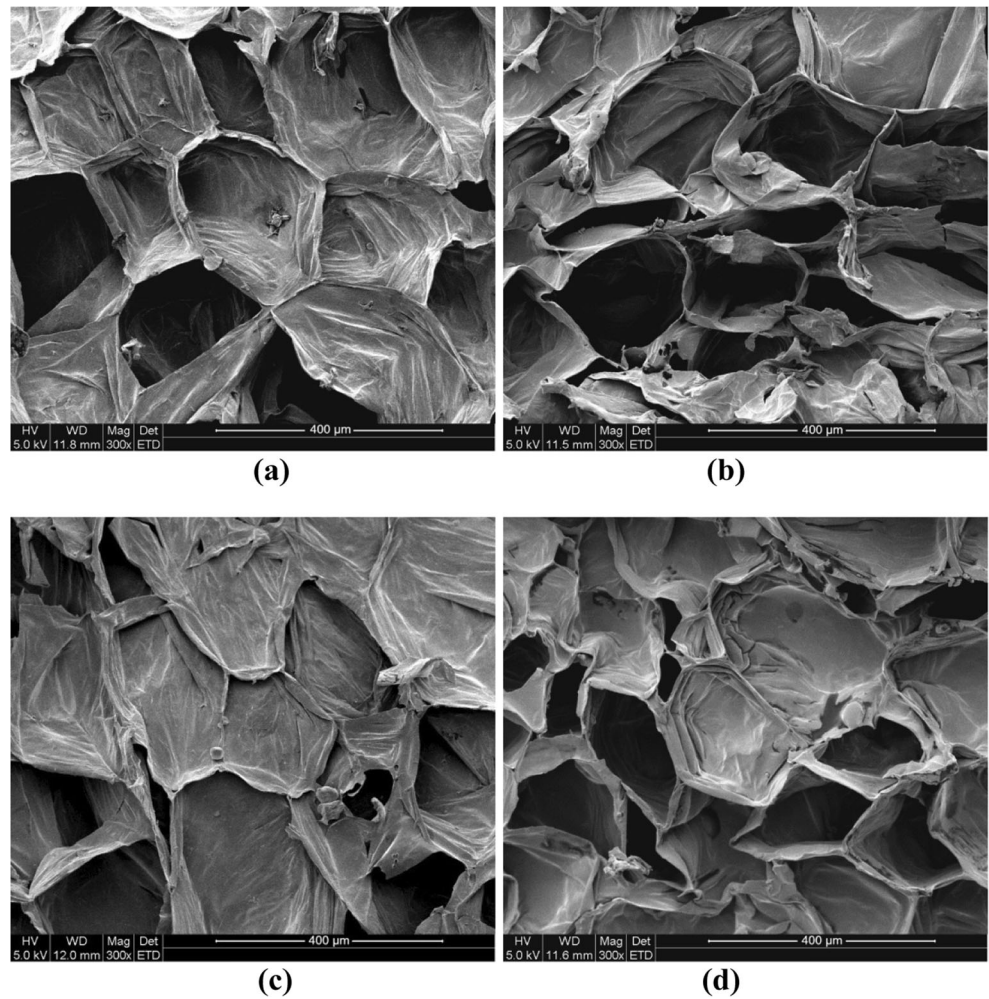
In the tissues of fruits and vegetables, total content of calcium can be mainly divided into two categories: bound calcium in the cell wall and free calcium in the intracellular tissue. The calcium bound in the cell wall is a key factor to protect the texture of fruits and vegetables. Chang et al. (1993) reported that the calcium content bound in the cell wall was the calcium content in AIS, due to the fact that free calcium ions were soluble in 80 % ethanol. Hence, investigation of the ratio between calcium content in AIS and total calcium content under different freezing conditions is very meaningful. The calcium in AIS/total calcium ratio of all the frozen samples significantly ($p<0.05$) decreased. This was because high water content of radish cylinder samples was inclined to form relatively large ice crystals during freezing, causing the cellular mechanical damage. This damage led to the release of the bound calcium as free calcium. Similar results had also been reported in the strawberries (Galletto et al. 2010) and broccoli (Xin et al. 2014b).

UAIF and UAIFW samples had significantly ($p<0.05$) higher ratio of bound calcium/total calcium than IF and IFW samples, respectively. In addition, UAIFW and IFW significantly ($p<0.05$) decreased the ratio of bound calcium/total calcium, compared to UAIF and IF, respectively. The results indicated that ultrasonic and unwrapped treatment maintained the ratio of bound calcium/total calcium. This was because the shorter corresponding freezing time (Fig. 1) for ultrasonic and unwrapped treatment, leading to the formation of smaller ice crystals (Fig. 4) and less destruction to the cell walls; thus, less bound calcium was lost during the thawing process.

Analysis of Microstructure

Figure 3 shows the microstructures of frozen radish cylinders under different freezing conditions by scanning electron microscopy (SEM). The pores observed in the frozen tissue of SEM images were associated with the size and location of ice crystals (Chevalier et al. 2000). The UAIF samples (Fig. 3c) appeared to be the most compact and dense with the smallest pores, indicating the formation of the smallest ice crystals during freezing process. Larger ice crystal pores can be observed in the IF (Fig. 3a) and UAIFW (Fig. 3d) samples, compared with the UAIF samples. The most and biggest pores were formed by the IFW (Fig. 3b). The results indicated that ultrasonic treatment can decrease the size of the ice crystals. This was due to the induction of ice nucleation to improve the freezing rate (Kiani et al. 2011; Xin et al. 2014a; Xu et al. 2014) and fragmentation of the pre-existing dendritic ice crystals into smaller nuclei to promote the secondary nucleation by ultrasonic treatment (Chow et al. 2003, 2005; Saclier et al. 2010). Additionally, the results also showed that the pores of wrapped samples were bigger. This was attributed to the

Fig. 3 Scanning electron micrographs of freeze-dried radish cylinders frozen by different freezing conditions. **a** IF, **b** IFW, **c** UAIF, **d** UAIFW



decrease of freezing rate by heat transfer insulation with wrapped treatment.

Analysis of Quality Attributes

The freezing and thawing losses of samples under different freezing conditions are shown in Fig. 4. The freezing loss was measured to evaluate the mass transfer during freezing process, while the thawing loss was tested to assess the quality change. It can be seen from this figure that significant differences ($p < 0.05$) of freezing loss were observed between wrapped and unwrapped radish samples. The freezing loss of IF and UAIF was quite higher than that of IFW and UAIFW. This was mainly because the polyethylene plastic wrap cut off the contact between coolant and samples. In theory, the ultrasound would improve the mass transfer during the osmosis process, but there were no significant ($p > 0.05$) differences of freezing loss between UAIF (1.32) and IF (1.36). This might be due to the fact that the mass transfer was not very strong under the very short freezing time (about

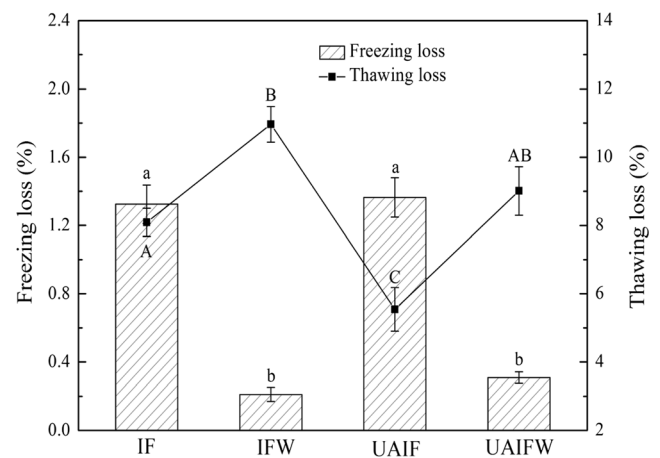


Fig. 4 Freezing and thawing losses of radish cylinders under different freezing conditions. Bars represent mean±standard deviation of triplicates. The different lower-case superscript letters (a, b) and capital superscript letters (A–C) indicate significant differences ($p < 0.05$) of freezing loss and thawing loss, respectively

13 min) and extremely low temperature circumstance ($-20\text{ }^{\circ}\text{C}$). Although the samples of IFW and UAIFW were not in direct contact with the coolant, the freezing loss still occurred. This was arising from the phenomenon of freezing weight loss during freezing process.

The thawing loss, which is the weight loss during the thawing process, is one of the most crucial indicator to evaluate the quality of frozen samples. Figure 4 shows that the thawing loss of UAIF was the lowest (5.54 %), followed by IF (8.09 %), and UAIFW (9.01 %), whereas that of IFW was the highest (10.96 %). The results indicated that ultrasonic and unwrapped treatment can decrease the thawing loss. Moreover, it was not hard to observe that the thawing loss was strictly consistent with the freezing time (Fig. 1). A number of factors affected the drip loss in terms of thawing rate, size and location of ice crystals, extent of water reabsorption, water-holding capacity, and nature of tissue of material (Islam et al. 2014). The higher the water content of food samples was, the more susceptible the large ice crystals formed during freezing process. This caused more drip loss and mechanical damage to the samples (Fernández et al. 2006). Since the radish contained high content of water, thawing loss was mainly attributed to ice crystals formed by cellular water. It can be concluded from the Fig. 3 that the ultrasonic and unwrapped treatment had the smaller ice crystal pores, which can explain the different thawing loss under different freezing conditions. In addition, the uptake of calcium from coolant CaCl_2 might also play a role in maintaining cell wall structure, contributing to the drip loss reduction (Table 1).

Firmness is a critical quality attribute of fruits and vegetables for the consumers' acceptability. The firmness values of radish cylinders under different freezing conditions are presented in Fig. 5. In view of the experimental circumstances, two crucial factors which affected the firmness were freezing rate and calcium content. Galetto et al. (2010) had reported

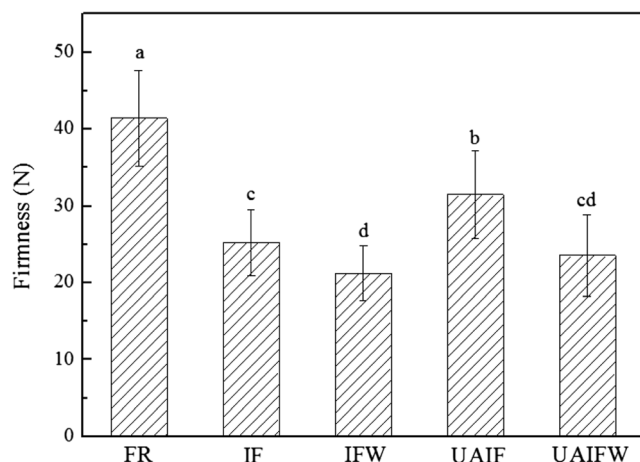


Fig. 5 The firmness of fresh and thawed radish cylinders frozen by different freezing conditions. Bars represent mean \pm standard deviation of triplicates. The different letters (a–d) indicate significant differences ($p < 0.05$)

that an irreversible turgor loss resulted from the process of freezing and thawing, but the calcium treatment prevented the fruit softness after freezing and thawing process. Awad et al. (2012) had reported that rapid freezing rates generated small ice crystals, while slow freezing rates induced the formation of large ice crystals, which damaged the physical structure (i.e., texture) and deteriorated the food quality. It can be observed from Fig. 5 that the firmness of all the frozen samples significantly ($p < 0.05$) decreased, compared to the fresh samples. This was because the damage effect of natural cellular structure from the formation of ice crystals was stronger than the protection effect from the increase of calcium content. Compared to the IFW and UAIFW samples, the samples subjected to UAIF and IF had significantly ($p < 0.05$) higher firmness. This was justified with the shorter freezing time (Fig. 1), smaller ice crystals, and better tissue structure (Fig. 3) and higher ratio bound calcium/total calcium (Table 1) of UAIF and IF samples.

Sensory evaluation of the fresh and frozen-thawed radish samples in terms of appearance, aroma, flavor, and texture are presented in Table 2. It can be seen that all the scores of descriptors of the thawed radish samples significantly ($p < 0.05$) decreased compared to the fresh samples. This was because the formation of ice crystals during the freezing process caused the irreversible microstructure changes and uncontrollable drip loss after thawing, resulting in the decrease of the appearance, flavor, and texture scores. In addition, from the results of our other studies (not show here), obvious differences of the volatile compounds between the fresh and thawed radish samples were observed. The most abundant compound of 4-isothiocyanato-1-(methylthio)-1-butene in red radish was also the most heavily affected compound after freezing and thawing process. The relative amount of this compound in the fresh samples was 38.10 % of total amount of volatiles (based on the peak area), while it remarkably increased to around 60 % in the frozen-thawed radish samples. This could be the reason why the aroma score declined. For the different freezing conditions, the UAIF was found to be superior than IF, IFW, and UAIFW in terms of appearance, aroma, and texture. This might be related to the shortest freezing time of UAIF, leading to less damages to cellular and tissue structures, less drip loss, and better preservation of firmness. Additionally, the flavor scores of IFW and UAIFW were higher than those of IF and UAIF. This was due to the fact that wrapped treatment prevented the coolant penetrating into the radish samples.

Water Distributions in Fresh and Thawed Radish Cylinders

The spin–spin relaxation times (T_2) were determined by LF-NMR analysis to describe the water status of the samples frozen by different freezing conditions. The description of water status included the mobility, distribution, position of

Table 2 Sensory evaluation of fresh and thawed radish cylinders under different freezing conditions

Treatments	FR	IF	IFW	UAIF	UAIFW
Appearance	23.0±1.2 ^a	20.8±1.3 ^b	19.4±1.4 ^c	21.2±1.2 ^b	19.1±1.3 ^c
Aroma	22.0±0.9 ^a	20.1±1.2 ^b	20.2±1.1 ^b	20.9±1.2 ^b	20.4±1.2 ^b
Flavor	24.0±1.5 ^a	21.0±1.2 ^c	23.2±1.7 ^b	21.5±0.9 ^c	23.5±0.9 ^b
Texture	24.0±1.1 ^a	19.9±1.1 ^b	18.1±1.3 ^c	20.4±1.1 ^b	17.7±1.3 ^c
Total score	93.0±1.2 ^a	81.8±1.2 ^{bc}	80.9±1.4 ^c	84.0±1.1 ^b	80.7±1.2 ^c

Values with different lowercase letters in the same row are significantly different ($p < 0.05$). Results are mean±standard deviation

the water, and interactions between water and macromolecules (Musse et al. 2010). The T_2 relaxation curves can be divided into three distinct regions from Fig. 6. Region I represents the water molecules (hydration monolayer water) bound to the product by strong H-bonds. Region II ascribes to the water molecules (multilayer water) strongly bound to the monolayer. Region III stands for the water molecules (“free” or solvent water) weakly bound to the product compared to those in regions I and II (Cheng et al. 2014a; Lagnika et al. 2013). Normally, the shortest transverse relaxation time T_{21} could be associated with the water contained in cell walls, resulting from chemical exchange effect by fast proton exchange between water and hydroxyl protons on the rigid cell wall polysaccharides (pectin, cellulose, and hemicellulose). The intermediate relaxing time T_{22} represents the water contained in cytoplasm, arising from chemical exchange between water and proteins of the cytoskeleton and enzymes and the high viscosity of the cytosol. The longest relaxation time T_{23} represents the water contained in the vacuole, due to the chemical exchange by slow proton exchange between water and sugars and other low weight compounds that constitute the dilute solution of the sap (Vicente et al. 2011).

Figure 6 shows the T_2 relaxation time distribution curves of fresh and frozen samples under different freezing conditions. The distribution of relaxation times in radish samples, T_2 (0–

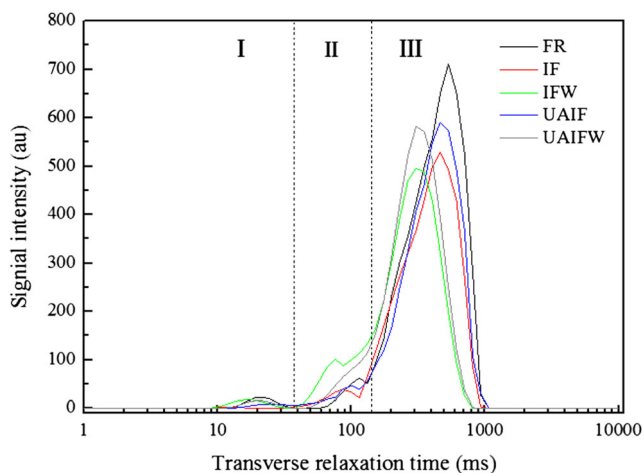


Fig. 6 Typical distribution of T_2 relaxation of fresh and thawed radish cylinders under different freezing conditions

37 ms) in region I, T_2 (37–151 ms) in region II, and T_2 (151–932 ms) in region III were assigned to water in the cell wall, cytoplasm water and extracellular, and vacuole, respectively. It can be observed from the figure that all the curves of frozen samples shifted toward the left, compared with the fresh samples. Kerr et al. (1997) had also reported that there was a significant decrease in the T_2 relaxation time of kiwifruit after the freezing–thawing process. As mentioned earlier, the shorter T_2 relaxation time is associated with the greater degree of bound hydrogen proton or the smaller freedom degree of hydrogen. This was probably related to the drip loss, resulting from the formation of ice crystal during the freezing process. The drip loss, which was the leakage of the water inside the samples, may improve the bound ability of water and reduce the freedom degree of hydrogen proton.

The relaxation times (T_{21} , T_{22} , and T_{23}) and relative area percentage under each peak (M_{21} , M_{22} , and M_{23}) for different radish samples are shown in Table 3. The results showed that ultrasonic and wrapped treatment significantly ($p < 0.05$) affected the mobility and distribution of water in radish cylinders. The frozen samples had significantly ($p < 0.05$) shorter relaxation times (T_2), compared to untreated samples. This decrease in T_2 values indicated an overall decrease in water mobility caused by freezing. The formation of the ice crystals during freezing process led to the damages of cell membranes and tonoplast, resulting in the water loss from the cytoplasm (T_{22}) and vacuole (T_{23}). The destruction of cell walls by ice crystals led to the chemical exchange between water and hydroxyl protons on the rigid cell wall polysaccharides (pectin, cellulose, and hemicellulose), giving rise to water loss from the cell walls (T_{21}). In addition, the relaxation times of UAIF and IF were significantly ($p < 0.05$) higher than those of UAIFW and IFW. This might be related to the freezing rate and ice crystal size.

It can be also seen from Table 3 that freezing process had significant ($p < 0.05$) effect on the relative areas (M_{21} , M_{22} , and M_{23}). Compared to FR samples, the M_{23} of the frozen samples under different freezing conditions significantly ($p < 0.05$) decreased, while the M_{21} and M_{22} were contrary. As described previously, the areas under each peak represented the populations of the water, namely, M_{21} (cell wall water), M_{22} (cytoplasm and extracellular water), and M_{23} (vacuole water),

Table 3 The relaxation times and relative areas of T_{21} , T_{22} , and T_{23} populations of fresh and thawed radish cylinders under different freezing conditions

Mode	T_2 (ms)			Area of T_2 (%)		
	T_{21}	T_{22}	T_{23}	M_{21}	M_{22}	M_{23}
FR	21.74±0.13 ^b	114.91±3.12 ^a	533.67±8.24 ^a	1.52±0.19 ^b	2.44±0.20 ^c	96.04±2.10 ^a
IF	12.33±0.21 ^d	86.97±2.43 ^c	403.70±7.59 ^c	3.09±0.21 ^a	5.57±0.33 ^b	91.34±2.78 ^c
IFW	16.29±0.09 ^c	75.65±1.16 ^d	305.38±9.16 ^c	3.49±0.65 ^a	8.02±0.32 ^a	88.49±3.25 ^d
UAIF	23.77±0.19 ^a	100.23±1.89 ^b	464.16±7.95 ^b	2.26±0.43 ^{ab}	3.53±0.19 ^{bc}	94.21±2.83 ^b
UAIFW	21.54±0.16 ^b	76.97±2.21 ^d	351.12±6.14 ^d	3.79±0.32 ^a	4.98±0.22 ^b	91.23±1.98 ^c

Values with different lowercase letters in the same column are significantly different ($p < 0.05$). Results are mean±standard deviation ($n=3$)

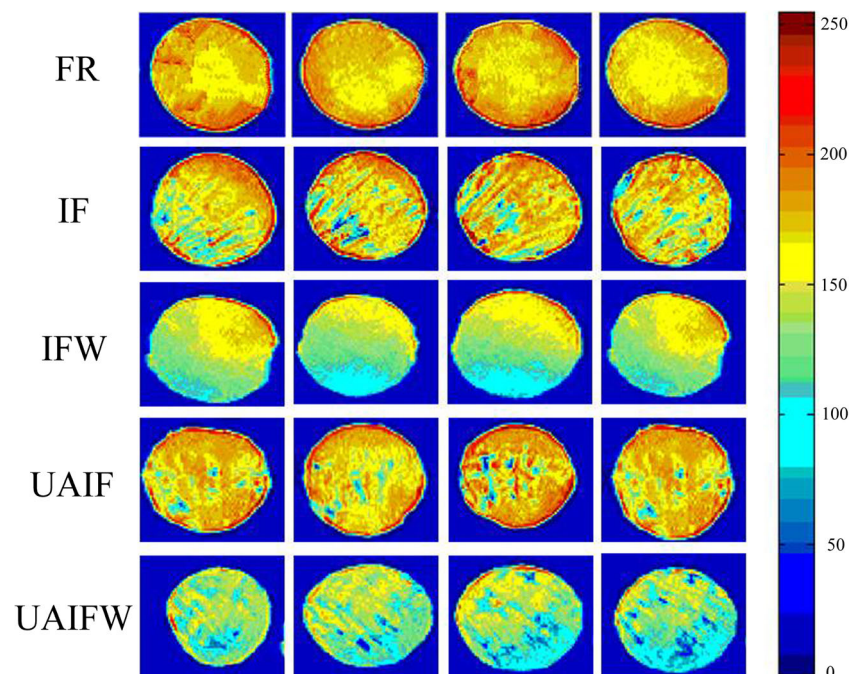
respectively. It indicated that the water loss was mainly from the vacuole during the freezing/thawing process. Under different freezing conditions, no significant ($p > 0.05$) differences of M_{21} were observed, while there were significant differences ($p < 0.05$) of M_{22} and M_{23} . This might be due to the fact that the percentage of water in the cell wall was extremely low. The water in the vacuole lost by the ice crystals leading to the decrease of M_{23} . These water from the vacuole possibly migrated into the cytoplasm and extracellular resulting in the increase of M_{22} . Moreover, the M_{23} of UAIF samples was significantly higher than that of IF, IFW, and UAIFW. This might be related to the smaller ice crystals (Fig. 3) and less drip loss (Fig. 4) for UAIF, compared to those three different conditions.

Figure 7 shows the MRI pseudocolor images of the water distributions at four different layers inside each sample. The water molecule content in the various zones of the sample is

directly proportional to the intensity of the signal (Marcone et al. 2013). Specifically, darker areas in an image indicate the presence of a more rigid structure with less water/protons. The area could contain a high concentration of ions or contrast agent, etc. which enhances relaxation, resulting in the darker area (Cheng et al. 2014a; Gussoni et al. 2007). As can be seen from this figure, the right color bar from the top to bottom represented the decrease of water content. It can be observed that the water distributions appeared distinctly different in these samples. The most red and yellow images of FR samples represented the highest free or mobile water. Compared to IF and UAIF, the images of IFW and UAIFW samples exhibited yellow, green, and cyan. It indicated that the water contents of IFW and UAIFW were lower than those of IF and UAIFW. This was consistent with the results of drip loss (Fig. 4).

In addition, the four images of FR samples displayed the most uniform on color. It represented that the water

Fig. 7 Water-selective transverse images of fresh and thawed radish cylinders under different freezing conditions at four different layers. Four pseudocolor images in the same row show the four different layers of 6-, 12-, 18-, 24-mm height of each radish cylinder, respectively



distributions at the different layers inside the FR samples were the most uniform. Similarly, the edge of each FR image showed an extremely red ribbon. It illustrated the water migration from the interior to the edge resulting from the pressure difference between the samples and the atmosphere. Similar results had been also reported on broccoli (Xin et al. 2013) and strawberry samples (Cheng et al. 2014a). IF images showed some small cyan regions, indicating that partial uneven water distributions existed in the IF samples. This might be attributed to the fact that the tissue damages by the formation of ice crystals during freezing process, leading to the water migration and gather in some regions. This water migration caused the relatively lower water content in other regions. The figure also depicts that the images of IFW and UAIFW were more uneven than those of IF and UAIF. It was implied that the water distributions were more uniform by ultrasonic treatment.

Conclusions

The results showed that ultrasonic and wrapped treatment during IF process had a significant ($p < 0.05$) effect on the freezing time, microstructures, calcium content, quality attributes, and water distributions of red radish. Ultrasonic treatment decreased the freezing time of red radish, leading to the formation of relatively smaller ice crystals with less damages to cellular and tissue structures, resulting in the reduction of drip loss and better preservation of firmness. The variation of the calcium content demonstrated that the wrapped treatment can effectively prevent the solutes penetrating into the radish samples. LF-NMR results quantified the effect of water migration in vacuole, cytoplasm and extracellular space, and cell wall of cells. MRI showed that the water content and uniformity of water distributions of all the frozen radish samples decreased, especially for the IFW samples. Results obtained from this study showed that ultrasonic treatment was a promising way to decrease the freezing time and possibly enhance the quality of frozen products. Moreover, the wrapped treatment can be an alternative method to prevent the solute uptake during IF process.

Acknowledgments The authors thank the financial support from China National Natural Science Foundation (Contract No. 21176104) and Ningbo (China) International Cooperation Project (Contract No. 2014D10016) which have enabled us to carry out this study.

References

Agnelli, M. E., & Mascheroni, R. H. (2002). Quality evaluation of food-stuffs frozen in a cryomechanical freezer. *Journal of Food Engineering*, 52(3), 257–263.

- Ahmad, S., Yaghmaee, P., & Durance, T. (2010). Optimization of dehydration of *Lactobacillus salivarius* using radiant energy vacuum. *Food and Bioprocess Technology*, 5(3), 1019–1027.
- Awad, T. S., Moharram, H. A., Shaltout, O. E., Asker, D., & Youssef, M. M. (2012). Applications of ultrasound in analysis, processing and quality control of food: a review. *Food Research International*, 48(2), 410–427.
- Bermúdez-Aguirre, D., Mobbs, T., & Barbosa-Cánovas, G. (2011). Ultrasound applications in food processing. In H. Feng, G. Barbosa-Canovas, & J. Weiss (Eds.), *Ultrasound technologies for food and bioprocessing* (pp. 65–105). New York: Springer.
- Chandrapala, J., Oliver, C. M., Kentish, S., & Ashokkumar, M. (2013). Use of power ultrasound to improve extraction and modify phase transitions in food processing. *Food Reviews International*, 29(1), 67–91.
- Chang, C. Y., Tsai, Y. R., & Chang, W. H. (1993). Models for the interactions between pectin molecules and other cell-wall constituents in vegetable tissues. *Food Chemistry*, 48(2), 145–157.
- Cheng, X.-f., Zhang, M., Adhikari, B., & Islam, M. N. (2014a). Effect of power ultrasound and pulsed vacuum treatments on the dehydration kinetics, distribution, and status of water in Osmotically dehydrated strawberry: a combined NMR and DSC Study. *Food and Bioprocess Technology*, 7(10), 2782–2792.
- Cheng, X.-f., Zhang, M., Adhikari, B., Islam, M. N., & Xu, B.-g. (2014b). Effect of ultrasound irradiation on some freezing parameters of ultrasound-assisted immersion freezing of strawberries. *International Journal of Refrigeration*, 44, 49–55.
- Chevalier, D., Sentissi, M., Havet, M., & Le Bael, A. (2000). Comparison of air-blast and pressure shift freezing on norway lobster quality. *Journal of Food Science*, 65, 329–333.
- Chow, R., Blindt, R., Chivers, R., & Povey, M. (2003). The sonocrystallisation of ice in sucrose solutions: primary and secondary nucleation. *Ultrasonics*, 41(8), 595–604.
- Chow, R., Blindt, R., Chivers, R., & Povey, M. (2005). A study on the primary and secondary nucleation of ice by power ultrasound. *Ultrasonics*, 43(4), 227–230.
- Chow, R., Blindt, R., Kamp, A., Grocutt, P., & Chivers, R. (2004). The microscopic visualisation of the sonocrystallisation of ice using a novel ultrasonic cold stage. *Ultrasonics Sonochemistry*, 11(3–4), 245–250.
- Comandini, P., Blanda, G., Soto-Caballero, M. C., Sala, V., Tylewicz, U., Mujica-Paz, H., Valdez Fragoso, A., & Gallina Toschi, T. (2013). Effects of power ultrasound on immersion freezing parameters of potatoes. *Innovative Food Science & Emerging Technologies*, 18, 120–125.
- Curtis, I. S. (2003). The noble radish: past, present and future. *Trends in Plant Science*, 8(7), 305–307.
- Delgado, A. E., & Rubiolo, A. C. (2005). Microstructural changes in strawberry after freezing and thawing processes. *LWT- Food Science and Technology*, 38(2), 135–142.
- Delgado, A. E., Zheng, L., & Sun, D.-W. (2009). Influence of Ultrasound on Freezing Rate of Immersion-frozen Apples. *Food and Bioprocess Technology*, 2(3), 263–270.
- Fernández, P. P., Otero, L., Guignon, B., & Sanz, P. D. (2006). High-pressure shift freezing versus high-pressure assisted freezing: Effects on the microstructure of a food model. *Food Hydrocolloids*, 20(4), 510–522.
- Galetto, C. D., Verdini, R. A., Zorrilla, S. E., & Rubiolo, A. C. (2010). Freezing of strawberries by immersion in CaCl_2 solutions. *Food Chemistry*, 123(2), 243–248.
- Gussoni, M., Greco, F., Vezzoli, A., Paleari, M. A., Moretti, V. M., Lanza, B., & Zetta, L. (2007). Osmotic and aging effects in caviar oocytes throughout water and lipid changes assessed by ^1H NMR T1 and T2 relaxation and MRI. *Magnetic Resonance Imaging*, 25(1), 117–128.
- Hajare, S. N., Dhokane, V. S., Shashidhar, R., Sharma, A., & Bandekar, J. R. (2006). Radiation Processing of Minimally Processed Carrot

- (Daucus carota) and Cucumber (Cucumis sativus) to Ensure Safety: Effect on Nutritional and Sensory Quality. *Journal of Food Science*, 71(3), S198–S203.
- Hu, F., Sun, D.-W., Gao, W., Zhang, Z., Zeng, X., & Han, Z. (2013a). Effects of pre-existing bubbles on ice nucleation and crystallization during ultrasound-assisted freezing of water and sucrose solution. *Innovative Food Science & Emerging Technologies*, 20, 161–166.
- Hu, S.-Q., Liu, G., Li, L., Li, Z.-X., & Hou, Y. (2013b). An improvement in the immersion freezing process for frozen dough via ultrasound irradiation. *Journal of Food Engineering*, 114(1), 22–28.
- Inada, T., Zhang, X., Yabe, A., & Kozawa, Y. (2001). Active control of phase change from supercooled water to ice by ultrasonic vibration 1. Control of freezing temperature. *International Journal of Heat and Mass Transfer*, 44(23), 4523–4531.
- Islam, M. N., Zhang, M., Adhikari, B., Xinfeng, C., & Xu, B.-g. (2014). The effect of ultrasound-assisted immersion freezing on selected physicochemical properties of mushrooms. *International Journal of Refrigeration*, 42, 121–133.
- Kawashima, L. M., & Valente Soares, L. M. (2003). Mineral profile of raw and cooked leafy vegetables consumed in Southern Brazil. *Journal of Food Composition and Analysis*, 16(5), 605–611.
- Kerr, W. L., Clark, C. J., McCarthy, M. J., & de Ropp, J. S. (1997). Freezing effects in fruit tissue of kiwifruit observed by magnetic resonance imaging. *Scientia Horticulturae*, 69(3–4), 169–179.
- Kiani, H., Sun, D.-W., Zhang, Z., Al-Rubeai, M., & Naciri, M. (2013a). Ultrasound-assisted freezing of *Lactobacillus plantarum* subsp. *plantarum*: The freezing process and cell viability. *Innovative Food Science & Emerging Technologies*, 18, 138–144.
- Kiani, H., Sun, D. W., Delgado, A., & Zhang, Z. (2012). Investigation of the effect of power ultrasound on the nucleation of water during freezing of agar gel samples in tubing vials. *Ultrasonics Sonochemistry*, 19(3), 576–581.
- Kiani, H., Zhang, Z., Delgado, A., & Sun, D.-W. (2011). Ultrasound assisted nucleation of some liquid and solid model foods during freezing. *Food Research International*, 44(9), 2915–2921.
- Kiani, H., Zhang, Z., & Sun, D.-W. (2013b). Effect of ultrasound irradiation on ice crystal size distribution in frozen agar gel samples. *Innovative Food Science & Emerging Technologies*, 18, 126–131.
- Lagnika, C., Zhang, M., & Mothibe, K. J. (2013). Effects of ultrasound and high pressure argon on physico-chemical properties of white mushrooms (*Agaricus bisporus*) during postharvest storage. *Postharvest Biology and Technology*, 82, 87–94.
- Li, B., & Sun, D.-W. (2002). Effect of power ultrasound on freezing rate during immersion freezing of potatoes. *Journal of Food Engineering*, 55(3), 277–282.
- Lucas, T., Flick, D., & Raoult-Wack, A. L. (1999). Mass and thermal behaviour of the food surface during immersion freezing. *Journal of Food Engineering*, 41, 23–32.
- Lucas, T., & Raoult-Wack, A. L. (1998). Immersion chilling and freezing in aqueous refrigerating media: review and future trends. *International Journal of Refrigeration*, 21(6), 419–429.
- Marcone, M. F., Wang, S., Albabish, W., Nie, S., Somnarain, D., & Hill, A. (2013). Diverse food-based applications of nuclear magnetic resonance (NMR) technology. *Food Research International*, 51(2), 729–747.
- Ming, L. C., Rahim, R. A., Wan, H. Y., & Ariff, A. B. (2009). Formulation of Protective Agents for Improvement of *Lactobacillus salivarius* I 24 Survival Rate Subjected to Freeze Drying for Production of Live Cells in Powderized Form. *Food and Bioprocess Technology*, 2(4), 431–436.
- Musse, M., Cambert, M., & Mariette, F. (2010). NMR Study of Water Distribution inside Tomato Cells: Effects of Water Stress. *Applied Magnetic Resonance*, 38(4), 455–469.
- Saclier, M., Peczalski, R., & Andrieu, J. (2010). A theoretical model for ice primary nucleation induced by acoustic cavitation. *Ultrasonics Sonochemistry*, 17(1), 98–105.
- Streit, F., Corrieu, G., & Béal, C. (2008). Effect of Centrifugation Conditions on the Cryotolerance of *Lactobacillus bulgaricus* CFL1. *Food and Bioprocess Technology*, 3(1), 36–42.
- Sun, D.-W., & Li, B. (2003). Microstructural change of potato tissues frozen by ultrasound-assisted immersion freezing. *Journal of Food Engineering*, 57(4), 337–345.
- Vicente, S., Nieto, A. B., Hodara, K., Castro, M. A., & Alzamora, S. M. (2011). Changes in Structure, Rheology, and Water Mobility of Apple Tissue Induced by Osmotic Dehydration with Glucose or Trehalose. *Food and Bioprocess Technology*, 5(8), 3075–3089.
- Xin, Y., Zhang, M., & Adhikari, B. (2013). Effect of trehalose and ultrasound-assisted osmotic dehydration on the state of water and glass transition temperature of broccoli (*Brassica oleracea* L. var. *botrytis* L.). *Journal of Food Engineering*, 119(3), 640–647.
- Xin, Y., Zhang, M., & Adhikari, B. (2014a). The effects of ultrasound-assisted freezing on the freezing time and quality of broccoli (*Brassica oleracea* L. var. *botrytis* L.) during immersion freezing. *International Journal of Refrigeration*, 41, 82–91.
- Xin, Y., Zhang, M., & Adhikari, B. (2014b). Ultrasound assisted immersion freezing of broccoli (*Brassica oleracea* L. var. *botrytis* L.). *Ultrasonics Sonochemistry*, 21(5), 1728–1735.
- Xu, B., Zhang, M., Bhandari, B., & Cheng, X. (2014). Influence of power ultrasound on ice nucleation of radish cylinders during ultrasound-assisted immersion freezing. *International Journal of Refrigeration*, 46, 1–8.
- Zheng, L., & Sun, D.-W. (2006). Innovative applications of power ultrasound during food freezing processes—a review. *Trends in Food Science & Technology*, 17(1), 16–23.